FLAASH, A MODTRAN4 ATMOSPHERIC CORRECTION PACKAGE FOR HYPERSPECTRAL DATA RETRIEVALS AND SIMULATIONS

S. Adler-Golden[1], A. Berk[1], L.S. Bernstein[1], S. Richtsmeier[1], P.K. Acharya[1], and M.W. Matthew[1],
G.P. Anderson[2], C. L. Allred[2], L.S. Jeong[2], and J.H. Chetwynd[2]

[1]Spectral Sciences, Inc.,
99 South Bedford St., Burlington, MA 01803

[2]Phillips Laboratory, Geophysics Directorate,
Hanscom AFB, MA 01731

1.   INTRODUCTION

FLAASH (Fast Line-of-sight Atmospheric Analysis of Spectral Hypercubes) is a MODTRAN-based "atmospheric correction" software package which is being developed by the Air Force Phillips Laboratory, Hanscom AFB and Spectral Sciences, Inc. to support current and planned IR-visible-UV hyperspectral and multispectral sensors. The main objectives are to provide (1) accurate, physics-based derivation of surface and atmospheric properties (such as surface albedo, surface altitude, water vapor column, aerosol and cloud optical depths, surface and atmospheric temperatures), (2) minimal computation time requirements, and (3) an interactive, user-friendly interface for running arbitrary MODTRAN calculations. FLAASH is written in the Interactive Data Language (IDL) (Research Systems, Inc., Boulder, CO) for compatibility with a wide variety of computer platforms and to facilitate its use with IDL-based display/analysis software such as ENVI.

FLAASH draws heavily on existing spectral analysis methods and codes that have been developed for both research and general use (e.g., Gao *et al.*, 1996; Green *et al.*, 1996; King *et al.*, 1992; Richter, 1996; Wan and Li, 1997). It is designed as a general-purpose code and is being developed in parallel with upgrades to MODTRAN in order to take advantage of the latest improvements in accuracy and speed. FLAASH is currently interfaced with a pre-release version of MODTRAN4 (Berk *et al.*, 1996). This paper briefly describes the progress achieved to date in the code development and presents some preliminary results. The initial version of FLAASH provides the following capabilities:

- Support for AVIRIS, HYDICE, and similar near-IR/visible/UV sensors;
- A graphical user interface for performing MODTRAN4 spectral calculations, including data simulations;
- Data-derived column water vapor and relative surface altitude (from column oxygen) image files and displays, and aerosol property retrieval capability based on known surface reflectances;
- Atmospherically corrected images (i.e., surface spectral reflectances) for non-thermal wavelengths (mid-IR through UV), including an image-sharpening adjacency effect correction.

The algorithm for deriving the surface and atmospheric properties utilizes the full MODTRAN4 accuracy and accounts for adjacency effects associated with atmospheric scattering. Compared to previous versions of MODTRAN, the new correlated-k radiation transport algorithm in MODTRAN4 (Berk *et al.*, 1994) provides improved accuracy in treating molecular absorption over scattering paths. In addition, an order of magnitude reduction in computation time is achieved by using MODTRAN4's lower resolution (15 cm^{-1}) option.

Brief descriptions of the computational approach and representative results of hyperspectral data analyses using FLAASH are presented below.

2. METHODOLOGY

As in other first-principles atmospheric correction codes, model simulations of the spectral radiance are performed for appropriate atmospheric and viewing conditions over a range of surface reflectances. The desired properties (reflectance, column water vapor, etc.) are derived from the spectral radiance at each image pixel using look-up tables that are generated from these simulations. To minimize the number of simulations (i.e., MODTRAN runs) required to generate the tables, a physics-based parameterization of the radiance-reflectance relationship is used. This relationship can vary across the scene due to variations in water vapor column density. Therefore, as in the ATREM code (Gao *et al.*, 1996) the water vapor column is first determined for each pixel, then the result is used as an input to the surface reflectance retrieval algorithm.

The initial version of FLAASH handles the mid-IR through UV wavelengths where thermal emission can be neglected. For this situation the spectral radiance L^* at a sensor pixel may be parameterized as (Staenz *et al.*, 1996; Vermote *et al.*, 1995; Williams *et al.*, 1992)

$$L^* = A\rho/(1-\rho_e S) + B\rho_e/(1-\rho_e S) + L^*_a \qquad (1)$$

where ρ is the pixel surface reflectance, ρ_e is an average surface reflectance for the surrounding region, S is the spherical albedo of the atmosphere, L^*_a is the radiance backscattered by the atmosphere, and A and B are coefficients that depend on atmospheric and geometric conditions. The first term in Equation (1) corresponds to the radiance from the surface that travels directly into the sensor, while the second term corresponds to the radiance from the surface that is scattered by the atmosphere into the sensor.

The values of A, B, S, and L^*_a may be determined empirically from MODTRAN spectral radiance calculations for three different spatially and spectrally uniform reflectances (such as $\rho=\rho_e=0$, 0.5, and 1.0). The backscattered radiance term L^*_a is simply the radiance for zero surface reflectance ($\rho=\rho_e=0$). The first (direct radiance) term is output by MODTRAN separately from the total radiance L^*; thus, the second (scattered radiance) term is isolated by subtracting the direct surface radiance and L^*_a from the total radiance. Equation (1) applies rigorously to monochromatic light. However, because S is small (of order 10^{-2} to 10^{-1} for clear sky) the radiance-reflectance relationship is sufficiently linear that Equation (1) accurately describes integrated in-band (i.e., sensor channel) radiances as well as true monochromatic radiance.

The spatially averaged reflectance ρ_e is used to account for "adjacency effects"--i.e., radiance contributions that, because of atmospheric scattering, originate from parts of the surface not in the direct line of sight. Strictly speaking, the ρ_e's in the numerator of the second term and in the denominators of the first and second terms are not identical. The former represents a weighted average over the surface region (typically around 1 km in width when viewed from a high-altitude sensor) that contributes to forward scattering from the ground into the sensor, while the latter represents an average over a larger region that contributes to the scattering back down to the ground. However, because S is small and the size of the averaging region is non-critical, the two averaged reflectances may be equated with little error.

The method for solving Equation (1) for the surface reflectance ρ in FLAASH parallels that in the ATCOR2 code (Richter, 1996) but differs in detail. The steps are as follows:

1. MODTRAN4 spectral radiance calculations for surface reflectances of 0, 0.5, and 1.0 are performed for a range of water vapor column densities to determine the Equation (1) parameters as a function of wavelength and water vapor column. The parameters for a spectral interval containing a selected water band are used to determine water vapor column densities for each pixel. The method, which is similar to the two-band method used in ATCOR2, involves comparisons of data and simulations for in-band and out-of-band radiance averages using a look-up table. The water column densities and the Equation (1) parameters for the entire wavelength region are stored for subsequent use.

2. A spatially averaged radiance image L^*_e is generated by convolving the radiance image L^* with a spatial weighting function appropriate for the sensor altitude, aerosol scale height, and aerosol scattering phase function.

3. From the resulting L^*_e an approximate ρ_e is generated from Equation (1) using ρ_e to represent all of the surface reflectances.

4. The resulting ρ_e is combined with the radiance L^* to solve Equation (1) for ρ.

To save computation time in processing the image, steps 3 and 4 are actually performed on a grid of trial L^*, L_e^*, wavelength, and water column values, and the resulting ρ values are entered into a 4-dimensional look-up table. The ρ calculation for each pixel is then carried out in a single step by interpolating between the table values.

The computation time consumed for a typical analysis of an 0.4-2.5 μm hyperspectral image on a 200-MHz personal computer is five minutes or less for the MODTRAN4 calculations (3 reflectances x 13 water vapor columns = 39 spectra, up to 36 atmospheric layers) plus around ten minutes for the image inversion (water column determination, spatial averaging, and generation of surface reflectance) for an AVIRIS 224-channel, 512x614-pixel image. Since the MODTRAN4 outputs are stored, they can be re-used to analyze a series of images taken under similar atmospheric conditions.

In addition to determining the water vapor column density, FLAASH derives pressure altitudes by applying the same method to the oxygen 762 nm absorption band. Because MODTRAN4's correlated-k algorithm more accurately represents molecular absorption in the presence of scattering, the water vapor and oxygen densities derived from FLAASH are expected to be more accurate than those obtained using previous versions of MODTRAN as well as from more approximate radiation transfer algorithms.

3. RESULTS

Several AVIRIS and HYDICE images have been used to test the initial FLAASH code. Some results are shown in Figures 1 through 4. The "US Standard" model atmosphere was assumed in the analyses.

Figure 1 shows a greyscale column water vapor map for Cuprite, Nevada derived from a 1994 AVIRIS image (No. PG02104). Outlines of visible features, including a north-south highway, are superimposed to guide the eye. Figure 2 shows corresponding maps of the surface altitude derived from the oxygen band (left) and the actual altitudes from US Geological survey data (right). All three images show two mountain ridges (dark regions) on either side of the highway that rise several hundred meters above a flat region to the southeast. The similarity between the Figure 1 and Figure 2 images reflects a strong correlation between the altitude and column water vapor, as would be expected for a water vapor altitude profile that is reasonably uniform across the scene.

A quantitative comparison between the O_2 band-derived surface altitudes and US Geological Survey data is made in Figure 3. Both the relative and absolute altitudes are accurate to around 200 m or better. Similar altitude precision from O_2 band data was reported in a study by Green *et al.* (1996) of a different AVIRIS scene. As the O_2 band actually measures air pressure, the absolute altitudes are sensitive to the local weather conditions. For relative altitudes the main source of error is spectral non-linearity of the reflectance in the O_2 band region, which varies with the type of terrain and is especially pronounced with vegetation. We expect that better accuracy will be obtained in the future by developing a background-subtraction or terrain-dependent correction procedure.

Figure 4 shows two greyscale images of visible reflectance derived from a 1994 AVIRIS image of Moffett Field, CA (No. PG02106). This scene, at the edge of San Francisco Bay, contains a wide variety of features such as buildings, pavement, surface vegetation, streams, and salt ponds. The left hand images shows the reflectance generated using the full method described in the previous section, while the right hand image shows the reflectance generated without accounting for adjacency effects. The difference in contrast is striking, and illustrates the importance of incorporating adjacency effects in atmospheric correction of variegated scenes.

We are currently analyzing HYDICE measurements of scenes containing spectrally calibrated targets. Comparisons of retrieved and known surface reflectances will be very useful for inferring aerosol properties, which are the major source of uncertainty in visible and UV surface reflectance retrievals for clear-sky conditions. Either calibrated targets or "dark" pixels (known to contain vegetation or water) can be compared with retrieved reflectances as an aerosol optical property is varied, the property being retrieved from the best fit. Aerosol properties which may be potentially retrieved (i.e., to which the comparisons are sensitive) include the optical depth, albedo, and scattering phase function (via the adjacency effect).

4. CONCLUSION

Development of FLAASH, a fast software package for atmospheric correction and modeling of hyperspectral images using MODTRAN4, has begun with a focus on sensors covering mid-IR through UV wavelengths. An initial version of the code has been developed for analysis of AVIRIS and HYDICE data. Future efforts will focus on accuracy evaluations, improvements to MODTRAN4, incorporation of a comprehensive library of reflectance spectra, incorporation of aerosol retrieval techniques, and extensions of FLAASH to additional sensors and to the thermal IR region.

5. ACKNOWLEDGEMENT

6. REFERENCES

Berk, A, L.S. Bernstein, D.C. Robertson, P.K. Acharya, G.P. Anderson, and J.H. Chetwynd, 1996, "MODTRAN Cloud and Multiple Scattering Upgrades with Application to AVIRIS," Summaries of the Sixth Annual JPL Airborne Earth Science Workshop, JPL Publication 96-4, Vol. 1, Pasadena, California, pp. 1-7.

Gao, B.-C., K.B. Heidebrecht, and A.F.H. Goetz, 1996, "Atmosphere Removal Program (ATREM) Version 2.0 Users Guide," Center for the Study of Earth from Space/CIRES, University of Colorado, Boulder, Colorado, 26 pages.

Green, R.O., D.A. Roberts, and J.E. Conel, 1996, "Characterization and Compensation of the Atmosphere for Inversion of AVIRIS Calibrated Radiance to Apparent Surface Reflectance," Summaries of the Sixth Annual JPL Airborne Earth Science Workshop, JPL Publication 96-4, Vol. 1, Pasadena, California, pp. 135-146.

King, M. D., Y. J. Kaufman, W. P. Menzel, and D. Tanre, 1992, "Remote Sensing of Cloud, Aerosol, and Water Vapor Properties from the Moderate Resolution Imaging Spectrometer (MODIS)," IEEE Transactions on Geoscience and Remote Sensing, Vol. 30, pp. 2-27.

Richter, R, "Atmospheric Correction of DAIS Hyperspectral Image Data," 1996, SPIE AEROSENSE '96 Conference, Orlando, FL, April 8-12, SPIE Proceedings, Vol. 2758.

Staenz, K., D.J. Williams, and B. Walker, 1996, "Surface Reflectance Retrieval from AVIRIS Data Using a Six-Dimensional Look-Up Table," Summaries of the Sixth Annual JPL Airborne Earth Science Workshop, March 4-8, 1996, JPL Publication 96-4, Vol. 1, Pasadena, California, pp. 223-229.

Vermote, E., D. Tanre, J.L. Deuze, M. Herman, and J.J. Morcrette, 1994, "Second Simulation of the Satellite Signal in the Solar Spectrum (6S)," 6S User Guide Version 6.0, NASA-GSFC, Greenbelt, Maryland, 134 pages.

Wan, Zhengming, and Z.-L. Li, 1997, "A Physics-Based Algorithm for Retrieving Land-Surface Emissivity and Temperature from EOS/MODIS Data," IEEE Transactions on Geoscience and Remote Sensing, Vol. 35, pp. 980-996.

Williams, D.J., A. Royer, N.T. O'Neill, S. Achal, and G. Weale, 1992, "Reflectance Extraction from CASI Spectra Using Radiative Transfer Simulations and a Rooftop Radiance Collector," Can. Journal of Remote Sensing, Vol. 18, pp. 251-261.

Figure 1. Column water vapor map for an AVIRIS image of Cuprite, NE. Darker regions denote lower water content. Outlines of visible features are superimposed for reference.

Figure 2. Altitude maps for the same image. Left: derived from the O_2 absorption band. Right: USGS data. Darker regions denote higher altitude.
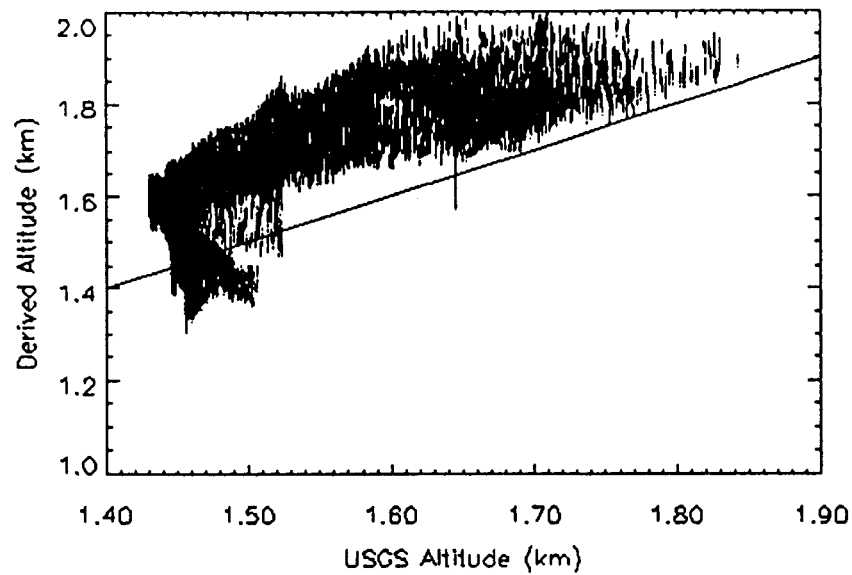
Figure 3. Comparison of actual (USGS) and derived surface altitudes for the Cuprite scene. Solid line denotes ideal agreement for the assumed US Standard model atmosphere.
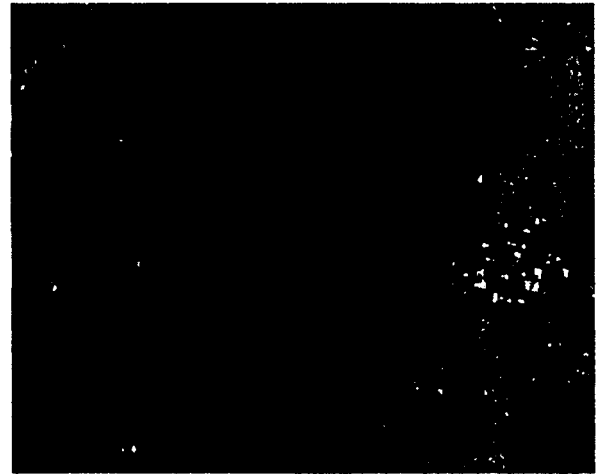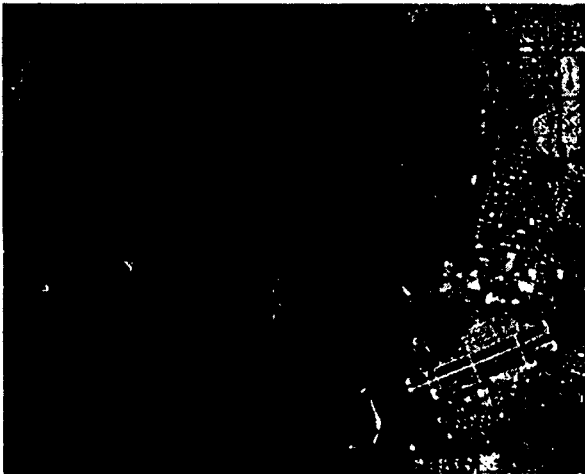

Figure 4. Derived reflectance images for AVIRIS Moffett Field scene with (left) and without (right) adjacency correction.